AFFDL-TR-68-150

A FINITE ELEMENT METHOD FOR THE PLASTIC BENDING ANALYSIS OF STRUCTURES

H. Armen, Jr.**
A. Pifko***
H. S. Levine**

Grumman Aircraft Engineering Corporation
Bethpage, L. I., New York

A finite element technique is presented for the plastic analysis of structures subjected to out-of-plane bending alone, or in combination with in-plane membrane stresses. The method makes use of a linear matrix equation of finite element analysis, formulated to include the effect of initial strains. This equation is applied to the plasticity problem by interpreting plastic strains as initial strains, the material nonlinearity being introduced through subsidiary stress-strain relations from an incremental plasticity theory. In addition, the analysis is combined with an incremental technique developed to account for the effects of geometric nonlinear behavior. Thus, the present analysis is capable of treating the combined effects of material and geometric nonlinearity. Application of the procedure is made to beam and arch structures in the presence of both types of nonlinearity, and to rectangular plates for which material nonlinearity alone is present.

This work sponsored by NASA under Contract NAS 1-7315

**Research Scientist
***Research Engineer

SECTION I

INTRODUCTION

The description of plastic behavior presents some basic difficulties to the structural analyst. These difficulties are associated with a proper description of the material phenomenon and the nonlinear nature of the resulting governing equation. Thus, the mathematical formulation of the plasticity problem makes an analysis of all but the simplest structures a very formidable, if not an impossible, task. Consequently, considerable attention has been given recently to the extension of finite element techniques to include the effects of plastic behavior (References 1-5). These techniques have the advantage of being capable of treating the effects of plasticity in complex structures by utilizing various algorithms for linearizing the basic nonlinear nature of the problem.

Most of the current effort concerned with the application of finite element techniques to the plasticity problem has been limited to the treatment of structures in states of membrane stress. In addition, the methods generally neglect the effects of geometric nonlinearity. These limitations are too restrictive for many important aerospace structures. Consequently, it is the purpose of the present paper to extend the methods already developed to provide for a plastic bending analysis that accounts for membrane stress states and geometric nonlinearity.

The present method makes use of a governing linear matrix equation that relates the applied loading to the nodal displacement and initial strains. For the purpose of a plasticity analysis, the plastic strains are interpreted as initial strains. Use of the initial strain concept, to treat the effects of plasticity, requires the development of appropriate matrix relations based on assumptions for the distribution of both displacements and initial (plastic) strain within a finite element. The specification of a distribution for plastic strain within a finite element forms the basis on which the present plasticity analysis depends.

Inclusion of the effects of geometric nonlinearity is primarily of concern in problems involving thin beams, plates, and shells in the plastic, as well as elastic, range. A finite element method that utilizes an incremental procedure requiring a successive modification of the element stiffness properties has been discussed in Reference 6. This method requires the introduction of an additional stiffness matrix to account for the effects on the bending

stiffness of the membrane stresses generated as a consequence of geometric nonlinearity. In addition, the effect that changes in geometry have on subsequent deformations is taken into account. This incremental procedure is incorporated into the plastic bending analysis to treat the combined effects of material and geometric nonlinearity.

SECTION II

MATERIAL NONLINEARITY-PLASTIC BENDING ANALYSIS

An important advantage of finite element techniques is the ability to specify the distribution of displacement and strain states within each finite element. This permits assumptions to be made for the distribution of plastic strain and the development of regions of plasticity within an element. These assumptions considerably reduce the complexity of the analysis by defining the distribution of plastic strain in any element, one the nodal values are determined. This feature is consistent with finite element analysis, and allows us to be concerned only with quantities at node points of the idealized structures.

For the case of membrane stress states, the plastic strains are assumed to vary in a prescribed manner in the plane of the element. For out-of-plane bending, an assumption must be made for the distribution of plastic strain through the thickness as well as in the middle surface of the element. Specifically, the present analysis assumes the plastic strains to vary linearly along the edges of a finite element between adjacent nodes, and in addition assumes a linear variation of plastic strains from the upper or lower surface of the element to an elastic-plastic boundary (or boundaries) located within the cross section of the element. These assumptions require the determination of the position of an elastic-plastic boundary based on its assumed distribution within the element during the course of loading. Thus, the present analysis utilizes the concept of a finite element in which there is a progressive development of a plastic region instead of the layered approach of Reference 7 or the sandwich idealization of Reference 8.

The above assumptions are made in the development of the governing linear matrix relation, which has been formulated to include the effects of initial strains. These assumptions, as applied to a typical beam finite element for which pure bending behavior has been assumed,

are shown in Figure 1. The function for the displacement in the z-direction is assumed to be of cubic order in the coordinate x, and is written in terms of the generalized nodal displacements as

$$w(x) = \left(1 - 3\frac{x^2}{\ell^2} + 2\frac{x^3}{\ell^3}\right) w_i + \left(3\frac{x^2}{\ell^2} - \frac{x^3}{\ell^3}\right) w_j + \left(x - 2\frac{x^2}{\ell} + \frac{x^3}{\ell^2}\right) w_{,x_i} + \left(\frac{x^3}{\ell^2} - \frac{x^2}{\ell}\right) w_{,x_j} \tag{1}$$

In choosing a displacement function, it is important to include all fundamental strained states and all rigid body terms. Equation 1 satisfies these requirements for a beam element, and allows for a constant shear load and linearly varying moment along the length of the element. The plastic strain distribution is assumed to vary linearly in the x-direction from its value at the upper (or lower) surface at node i, represented in Figure 1 as ϵ_{0i}, to its value at the upper (or lower) surface at node j, represented as ϵ_{0j}. This assumed distribution is written as

$$\epsilon = \left(\frac{z - \bar{z}}{t - \bar{z}}\right)\left[\epsilon_{0i}\left(1 - \frac{x}{\ell}\right) + \epsilon_{0j}\left(\frac{x}{\ell}\right)\right] \tag{2}$$

where $\bar{z}$ represents the depth of the elastic-plastic boundary. In addition, as seen from Equation 2, it is assumed that at a node, the plastic strain varies linearly from its value at the upper or lower surface to zero at an elastic-plastic boundary located through the cross section.

The depth of the elastic-plastic boundary, which propagates from the upper and lower surface, is measured from the neutral axis for pure bending, as shown in Figure 1. In general, the depth of this boundary cannot be directly related to the load. Hence, the value of $\bar{z}$ must be determined from the total strain distribution, which is assumed to vary linearly through the thickness in accordance with Kirchoff's hypothesis. The functional form representing the distribution of the elastic-plastic boundary is assumed to be a linear function of the coordinate x and may be written as

$$\bar{z} = \left(\bar{z}_j - \bar{z}_i\right)\left(\frac{x}{\ell}\right) + \bar{z}_i \tag{3}$$

where $\bar{z}_i$ and $\bar{z}_j$ represent the depth of the elastic-plastic boundary at nodes i and j, respectively. Thus, with the preceding assumptions, the elastic-plastic boundary consists of a surface in the interior of the element that extends over the entire area of the element and intersects the edges along straight lines joining nodes, as illustrated in Figure 1. In addition,

these assumptions eliminate the necessity of determining an elastic-plastic boundary on the faces of the element between nodes, but still require locating such a boundary through the thickness.

The present assumptions are further extended to include the effects of bending in combination with a membrane stress state. As seen in Figure 2, this extension necessitates the determination of the position of the elastic-plastic boundary relative to both the upper and/or lower surface. The functional representation of the plastic strain distribution and the representation of the elastic-plastic boundary are taken similar to Equations 2 and 3 written for both the upper and lower surface. A second matrix, in addition to the usual stiffness matrix, termed the initial stress stiffness matrix (to be discussed in the next section), is also implemented to account for the effects of the membrane load on the bending stiffness. This problem also requires the introduction of a second displacement component, u, acting in the axial direction,

$$u(x) = \left(1 - \frac{x}{\ell}\right) u_i + \left(\frac{x}{\ell}\right) u_j \tag{4}$$

It should be noted that although the functional form of the plastic strain distribution, as shown in Figure 2, does assume the existence of a neutral axis located within the cross section of the beam element, the present analysis is capable of considering plastic sections in which the neutral axis is not located within the thickness of the beam; that is, the upper and lower strains are of the same sign. This situation occurs with the application, or generation, of large membrane stresses as compared to the existing bending stresses. The treatment of this situation is accomplished by modifying the functional form of the plastic strain distribution given in Figure 2.

The present method has also been extended to treat the more complex problem of the plastic bending of a plate. A typical rectangular plate element is shown in Figure 3. The displacement function chosen is the one originally used by Bogner, Fox, and Schmit (Reference 9), and is in terms of products of first order Hermitian polynomials. The components of initial strain are assumed to vary as products of zero order Hermitian polynomials in the plane of the element and linearly through the cross section from their values at the upper (or lower) surface to zero at the elastic-plastic boundary. The depth of the boundary through

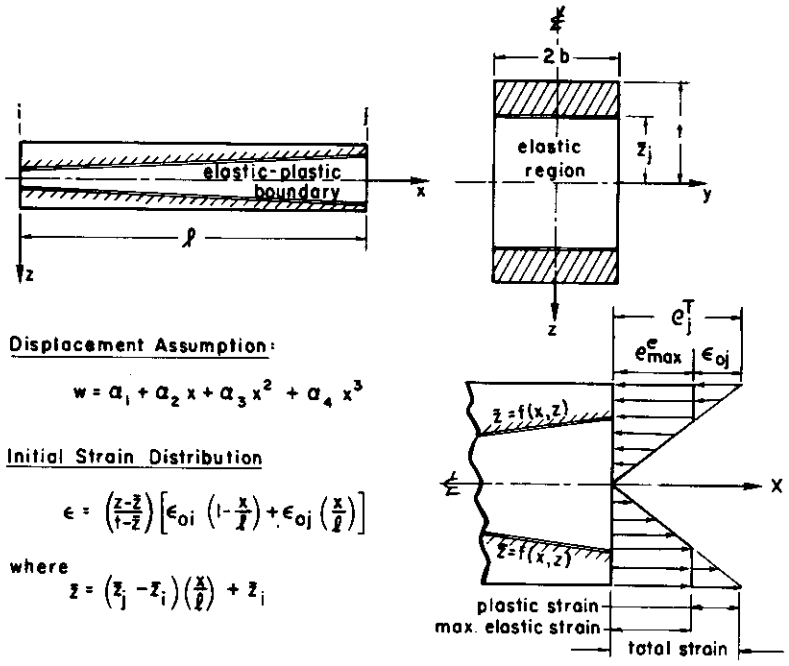

Displacement Assumption:

$$w = \alpha_1 + \alpha_2 x + \alpha_3 x^2 + \alpha_4 x^3$$

Initial Strain Distribution

$$\epsilon = \left(\frac{z-\bar{z}}{t-\bar{z}}\right)\left[\epsilon_{oi}\left(1-\frac{x}{\ell}\right)+\epsilon_{oj}\left(\frac{x}{\ell}\right)\right]$$

where

$$\bar{z} = \left(\bar{z}_j - \bar{z}_i\right)\left(\frac{x}{\ell}\right) + \bar{z}_i$$

Figure 1. Typical Elastic-Plastic Beam Element (Pure Bending)

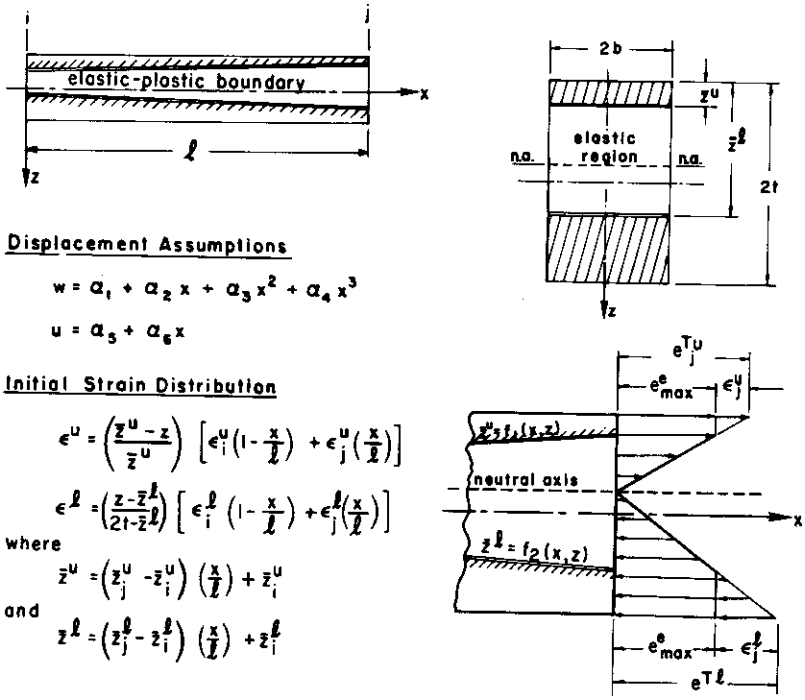

Displacement Assumptions

$$w = \alpha_1 + \alpha_2 x + \alpha_3 x^2 + \alpha_4 x^3$$

$$u = \alpha_5 + \alpha_6 x$$

Initial Strain Distribution

$$\epsilon^u = \left(\frac{\bar{z}^u - z}{\bar{z}^u}\right)\left[\epsilon_i^u\left(1-\frac{x}{\ell}\right)+\epsilon_j^u\left(\frac{x}{\ell}\right)\right]$$

$$\epsilon^\ell = \left(\frac{z-\bar{z}^\ell}{2t-\bar{z}^\ell}\right)\left[\epsilon_i^\ell\left(1-\frac{x}{\ell}\right)+\epsilon_j^\ell\left(\frac{x}{\ell}\right)\right]$$

where

$$\bar{z}^u = \left(\bar{z}_j^u - \bar{z}_i^u\right)\left(\frac{x}{\ell}\right) + \bar{z}_i^u$$

and

$$\bar{z}^\ell = \left(\bar{z}_j^\ell - \bar{z}_i^\ell\right)\left(\frac{x}{\ell}\right) + \bar{z}_i^\ell$$

Figure 2. Typical Elastic-Plastic Beam Element (Bending and Axial Loads)

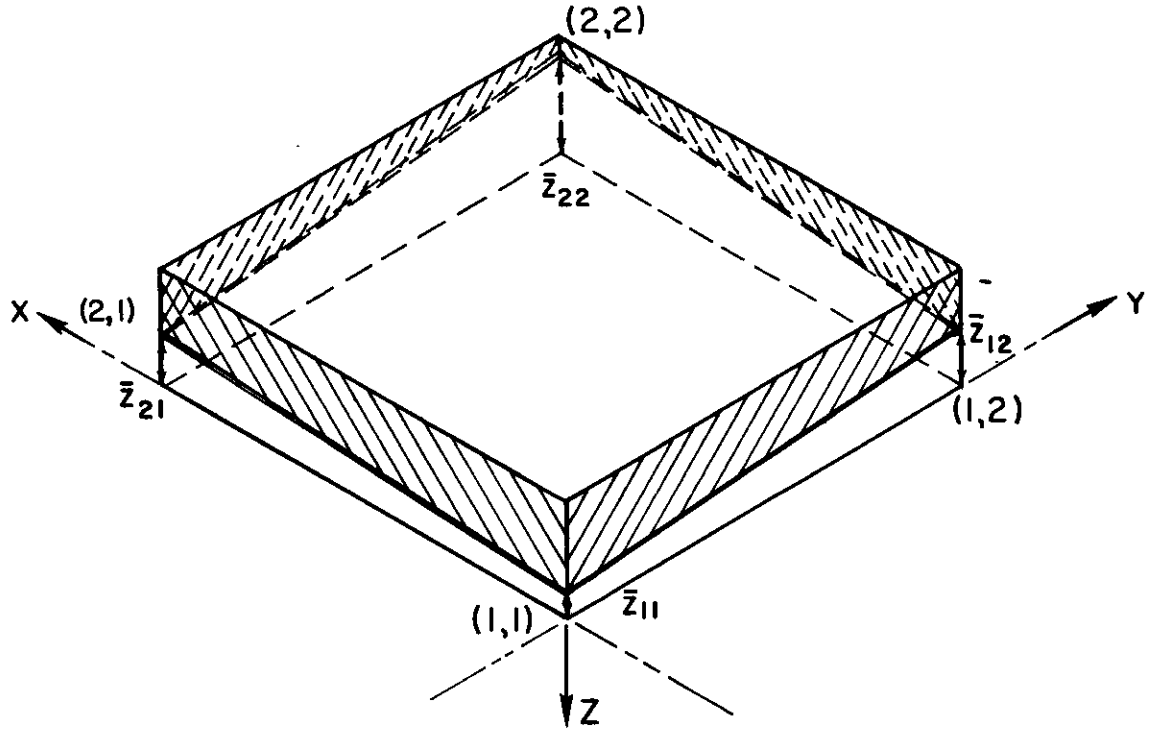

Displacement Assumption:

$$w = \sum_{i=1}^{2}\sum_{j=1}^{2}\left[H_{oi}^{(1)}(x)H_{oj}^{(1)}(y)W_{ij} + H_{1i}^{(1)}(x)H_{oj}^{(1)}(y)W_{,xij} + H_{oi}^{(1)}(x)H_{1j}^{(1)}(y)W_{,yij} + H_{1i}^{(1)}H_{1j}^{(1)}(y)W_{,xyij}\right]$$

Initial Strain Distribution:

$$\epsilon(x,y,z) = \left(\frac{z-\bar{z}}{t-\bar{z}}\right)\sum_{i=1}^{2}\sum_{j=1}^{2}H_{oi}^{(0)}(x)H_{oj}^{(0)}(y)\epsilon_{ij}$$

Elastic-Plastic Boundary:

$$\bar{z}(x,y) = \sum_{i=1}^{2}\sum_{j=1}^{2}H_{oi}^{(0)}(x)H_{oj}^{(0)}(y)\bar{z}_{ij}$$

Figure 3. Typical Elastic-Plastic Rectangular Plate Element (Pure Bending)

the thickness, which must be determined at each of the four nodes of the rectangular element, is computed from the total strains by means of the following relation:

$$\bar{z}_{ij} = \frac{\sigma_{yeild}}{\sqrt{(J_{2\,max})_{ij}}} \quad i,j = 1,2$$

where

$$(J_{2\,max})_{ij} = \frac{E^2}{(1+\nu)^2}\left[\left(e_x^T - e_y^T\right)^2 + e_x^T e_y^T + \frac{3}{4}\left(\gamma_{xy}^T\right)^2 + \frac{\nu}{(1-\nu)^2}\left(e_x^T - e_y^T\right)^2\right]_{ij}$$

and the superscript T denotes total strains. The function defining the elastic-plastic boundary in the plane of the element is assumed to be in the form of products of zero order Hermitian polynomials as shown in Figure 3. The foregoing assumptions associated with the plastic strain distribution and the representation of the elastic-plastic boundary ensure compatibility of these quantities along element boundaries.

METHOD OF ANALYSIS

Once the assumption is made on the distribution of displacement, the total strain distribution can be expressed in terms of nodal displacements by making use of the appropriate strain displacement relations in conjunction with the assumed displacement function. This relation can be written in matrix form as follows:

$$e^T = W\, d_0 \tag{5}$$

where e^T is the vector of total strains

d_0 is the vector of generalized nodal displacements.

The assumed distribution of plastic strains can be written in terms of their nodal quantities as

$$\epsilon = W_P\, \epsilon_0 \tag{6}$$

where ϵ_0 is the vector of nodal plastic strains.

The matrices $\mathbf{W}$ and $\mathbf{W}_p$ are, in general, functional matrices which depend explicitly on the assumptions made for the distribution of displacement and initial strain, respectively, within the element. Specifically, the assumptions discussed above for the beam and plate elements are used in the formation of $\mathbf{W}$ and $\mathbf{W}_p$ in the present analysis. The element stiffness properties in the presence of initial strains are developed on the basis of these two functional matrices. They are obtained by substituting Equations 5 and 6 into the expression for strain energy and then employing Castigliano's first theorem. To this end, the expression for strain energy which explicitly contains the effect of initial strains may be written as

$$U = \frac{1}{2} \iiint_V \mathbf{e}^{T'} \mathbf{E}\, \mathbf{e}^{T}\, dV - \iiint_V \mathbf{e}^{T'} \mathbf{E}\, \epsilon\, dV \tag{7}$$

where the elements of the matrix $\mathbf{E}$ are the coefficients associated with the appropriate linear stress strain relations. Substitution of Equation 5 and the assumed plastic strain distribution of Equation 6 into Equation 7 leads to

$$U = \frac{1}{2} \mathbf{d}_0' \mathbf{k}\, \mathbf{d}_0 - \mathbf{d}_0' \mathbf{k}^* \epsilon_0 \tag{8}$$

where

$$\mathbf{k} = \iiint_V \mathbf{W}' \mathbf{E}\, \mathbf{W}\, dV \tag{9}$$

$$\mathbf{k}^* = \iiint_{V_p} \mathbf{W}' \mathbf{E}\, \mathbf{W}_p\, dV \tag{10}$$

The matrix $\mathbf{k}$ represents the element elastic stiffness matrix and depends only on the assumption made for element displacements. The second integral, Equation 10, represents the initial strain stiffness matrix which is dependent on the assumptions for both total and plastic strains. The quantity V_p in Equation 10 is the volume of the plastic region in each element as determined by the representation of the elastic-plastic boundary. Consequently, the elements of the initial strain stiffness matrix $\mathbf{k}^*$ will be a function of, among other quantities, the depth of the elastic-plastic boundary at each node, and must therefore be continuously computed during the course of loading. The initial strain matrix for the beam element subjected to pure bending and that for combined bending and axial load are given in the Appendix. Due to space limitations the initial strain matrix associated with the rectangular plate bending element is omitted here. It may be found in Reference 14.

Application of Castigliano's theorem to Equation 7 yields the governing linear matrix equation for an individual finite element

$$\frac{dU}{d\,d_0} = P_0 = k\,d_0 - k^*\,\epsilon_0 \tag{11}$$

where P_0 is the vector of generalized nodal forces.

A similar equation is also developed in incremental form in anticipation of combining plasticity with the incremental geometric nonlinear analysis. This equation is written as follows:

$$\Delta P_0 = k\,\Delta d_0 - \bar{k}\,\Delta\epsilon_0 \tag{12}$$

It should be emphasized that the initial strain matrix associated with the increment of plastic strain $\Delta\epsilon_0$ in Equation 12 is written as $\bar{k}$ to distinguish it from the inital strain matrix k^* associated with the total plastic strain ϵ_0. These matrices may differ substantially, since the functional form assumed for the distribution of total plastic strain will not, in general, coincide with the assumed distribution associated with the increment of plastic strain. In the present analysis, ϵ_0 was assumed to vary linearly through the thickness from the upper and/or lower surface to the elastic-plastic boundary. This assumption implies a bilinear distribution of $\Delta\epsilon_0$. The specification of a distribution of this form requires the determination of a value of the plastic strain increment at some intermediate point in the cross section, in addition to a value at the upper and/or lower surface.

To avoid the added complexities associated with the use of Equation 12, we may alternatively use an incremental form of Equation 11 as follows:

$$\Delta P_0^i = k\,\Delta d_0^i - \Delta q^i \tag{13}$$

where

$$\Delta q^i = \Delta\left(k^{*^i}\,\epsilon_0^{\,i}\right) = k^{*^i}\,\epsilon_0^{\,i} - k^{*^{i-1}}\,\epsilon_0^{\,i-1}$$

and the superscripts i and i-1 refer to the current and preceding loading step, respectively. In Equation 13, the product of the initial strain matrix and the total plastic strain is considered as a vector of fictitious loads. The increment of this fictitious load, represented as Δq, is determined at any step by subtracting its current value from that computed in the

preceding step. In this manner, only total values of plastic strain are utilized in the governing linear matrix equation. The desired form of the equation is obtained by grouping the increments of generalized nodal forces and fictitious forces, resulting in the following equation:

$$k\ \Delta d_0^i = \Delta P^i + \Delta q^{i-1} \tag{14}$$

Here, it is seen that the values of the increment of fictitious load introduced into Equation 14 are values taken to be equal to those computed in the preceding load increment. The use of this type of predictor procedure is necessary because the depth of the elastic-plastic boundary (and the current value of plastic strain) at those nodes of the structure in the plastic range can be determined, in general, only from the stress (or strain) distribution computed at the end of the load step. The position of the elastic-plastic boundary is determined at the end of each load increment, and is assumed to remain fixed during the next increment.

Equation 14 is written for each element in the structural idealization and then appropriately assembled to form the overall linear matrix equation for the entire structure. This equation, not shown here, is identical in form to Equation 14. The incremental solution technique using this equation reduces to a sequence of linear problems in which the applied loading is constantly modified by the fictitious force vector.

PLASTICITY RELATIONS

The foregoing matrix equations must be used in conjunction with an appropriate plasticity theory. Plasticity is introduced into Equation 14 through subsidiary stress-strain relations provided by this theory. In the present paper, consideration is given to both elastic, strain-hardening or ideally plastic material behavior. For both types of behavior, the total strain increment at a node can be written as the sum of an elastic and plastic component, represented as Δe_0^e and $\Delta \epsilon_0$, respectively, in the following equation:

$$\Delta e_0^T = \Delta e_0^e + \Delta \epsilon_0 \tag{15}$$

In addition, the increment of elastic strain is related to the stress increment, $\Delta \sigma$, by means of Hooke's Law. Thus, Equation 15 can be written as

$$\Delta e^T = E^{-1}\ \Delta \sigma + \Delta \epsilon \tag{16}$$

For an elastic, strain-hardening material, we make use of a linear incremental relation between plastic strain and stress increment

$$\Delta \epsilon = C \quad \Delta \sigma \tag{17}$$

This relationship is represented in a general form by the matrix C in Equation 17. The formulation of this matrix is directly related to the plasticity theory chosen for use, i.e., these elements may be determined by using an isotropic hardening theory or the kinematic hardening theory of plasticity. The elements of this array for plane stress, obtained by using Drucker's postulate with the Prager-Ziegler kinematic hardening theory, are explicitly given in Reference 1.

Substituting Equation 17 into Equation 16 leads to an incremental stress-strain relation given in the Equation 18

$$\Delta \sigma = R^{-1} \quad \Delta e^{T} \tag{18}$$

where

$$R \equiv E^{-1} + C$$

It should be noted that there is no unique stress increment for a given plastic strain increment vector. Therefore, the matrix C, given in Reference 1, is singular. However, the matrix R, defined in Equation 18, will possess an inverse, thereby providing the necessary coefficients relating the stress increment to the increment of total strain.

The increment in total strain at a node, Δe_0^T, is obtained from the increment of displacement by using Equation 5 in incremental form as follows:

$$\Delta e_0^T = W_0 \quad \Delta d_0 \tag{19}$$

where W_0 is defined at a node. It should be noted from Equations 19 and 5 that the functional form chosen to represent the increment of total strain, Δe_0^T, is identical to that used in the representation of its full value, e_0^T. Thus, having obtained the increment of displacement from the solution of the total linear matrix equation in the form of Equation 14, Equations 15 through 19 represent the necessary relations that must be used to obtain the complete solution for increments of stress and strain, assuming elastic strain-hardening material behavior. After summing all incremental quantities, a new value of the increment of fictitious load, Δq, is determined for each element in the plastic range and the procedure is repeated until the desired maximum value of the load is reached.

Consideration of elastic, ideally plastic material behavior is necessary for predicting the collapse load of a given structure and loading situation. The two conditions to be satisfied for multiaxial elastic, ideally plastic material behavior are:

1) the stress increment vector must remain tangent to the loading surface, and

2) the plastic strain increment vector must remain normal to the loading surface, where the loading function is the representation, in stress space, of the initial yield function, or the subsequent yield function after some plastic deformation has occurred.

The above conditions are expressed analytically for the case of plane stress and using the von Mises yield condition by the following two equations:

$$(\sigma_x - \tfrac{1}{2}\sigma_y)\,d\sigma_x + (\sigma_y - \tfrac{1}{2}\sigma_x)\,d\sigma_y + 3\tau_{xy}\,d\tau_{xy} = 0 \tag{20}$$

$$\frac{d\epsilon_x}{(\sigma_x - \frac{1}{2}\sigma_y)} = \frac{d\epsilon_y}{(\sigma_y - \frac{1}{2}\sigma_x)} = \frac{d\gamma_{xy}^{p}}{3\tau_{xy}} = d\lambda \tag{21}$$

where $d\lambda$ is a positive scalar quantity.

If we consider the differential of the stress components as incremental quantities, the implicity differential of Equation 20 provides a linear relation among the components of stress increment, represented in matrix form as follows:

$$\Delta\boldsymbol{\sigma} = \bar{\mathbf{E}}\ \Delta\boldsymbol{\sigma} \tag{22}$$

Expressing $\Delta\sigma_x$ in terms of $\Delta\sigma_y$ and $\Delta\tau_{xy}$, yields the elements of the matrix $\bar{\mathbf{E}}$ as

$$\bar{\mathbf{E}} = \begin{bmatrix} 0 & -M_1 & -M_2 \\ 0 & 1 & 0 \\ 0 & 0 & 1 \end{bmatrix}$$

where

$$M_1 = (\sigma_y - \tfrac{1}{2}\sigma_x)/(\sigma_x - \tfrac{1}{2}\sigma_y)$$

$$M_2 = 3\tau_{xy}/(\sigma_x - \tfrac{1}{2}\sigma_y)$$

If we replace $d\epsilon_{ij}$ by $\Delta\epsilon_{ij}$, Equation 17 provides a linear relation between components of plastic strain increment, written as

$$\Delta\boldsymbol{\epsilon} = \tilde{\mathbf{E}}\ \Delta\boldsymbol{\epsilon} \tag{23}$$

Then expressing $\Delta\epsilon_y$ and $\Delta\gamma^p_{xy}$ in terms of $\Delta\epsilon_x$ gives the elements of the matrix $\tilde{E}$.

$$\tilde{\mathbf{E}} = \begin{bmatrix} 1 & 0 & 0 \\ M_1 & 0 & 0 \\ M_2 & 0 & 0 \end{bmatrix}$$

It is apparent from Equations 20 and 21 that only two of the three components of stress increment and only one of the three components of plastic strain increment are required to obtain the remaining components. Thus, only three of the six quantities are independent variables. The increments of stress and plastic strain can now be written in terms of a vector, $\Delta\boldsymbol{\omega}$, representing these independent quantities, arbitrarily chosen as $\Delta\epsilon_x$, $\Delta\sigma_y$, and $\Delta\tau_{xy}$,

$$\Delta\boldsymbol{\omega} = \begin{Bmatrix} \Delta\epsilon_x \\ \Delta\sigma_y \\ \Delta\tau_{xy} \end{Bmatrix} \tag{24}$$

Equations 22 and 23 may now be rewritten to relate the increments of stress and plastic strain in terms of $\Delta\boldsymbol{\omega}$

$$\Delta\boldsymbol{\sigma} = \bar{\mathbf{E}}\ \Delta\boldsymbol{\omega} \tag{25}$$

and

$$\Delta\boldsymbol{\epsilon} = \tilde{\mathbf{E}}\ \Delta\boldsymbol{\omega} \tag{26}$$

A relation between the vector $\Delta\boldsymbol{\omega}$ and the increment of total strain is obtained by substituting Equations 25 and 26 into Equation 16.

$$\Delta\boldsymbol{\epsilon}^T = \mathbf{E}^*\ \Delta\boldsymbol{\omega} \tag{27}$$

where

$$\mathbf{E}^* \equiv \mathbf{E}^{-1}\ \bar{\mathbf{E}} + \tilde{\mathbf{E}}$$

Once again, as in the case of strain hardening behavior, increments of displacement and total strain are obtained from the linear matrix equations. The solution for $\Delta\boldsymbol{\omega}$ from Equation 27 and its substitution into Equations 25 and 26 represent the procedure necessary to obtain the complete solution for displacements, stresses, and strains for any increment, assuming elastic, ideally plastic material behavior.

SECTION III

MATERIAL AND GEOMETRIC NONLINEARITY

For the preceding theory and applications, it was assumed that the strain-displacement relations were linear although the stress-strain law was not. The implementation of a nonlinear stress-strain relation for the characterization of material behavior merely depends on the absolute magnitudes of the elongations and shears existing in a body. When they exceed a certain value, nonlinear material characteristics become important and must be included to gain an insight into the response of the structure to further loading. Although the magnitudes of the shears and elongations may be sufficiently large to necessitate the inclusion of plastic effects, their values and the value of the angles of rotation may still be small compared to unity. If this condition, and the additional condition that the squares and products of angles of rotation may be neglected as compared to the elongations and shears remain valid, then the use of linear strain-displacement relations is justified. Thus, material nonlinearity can exist independently of geometric nonlinearity.

For flexible bodies (beams, plates, shells), the second condition (that on the squares and products of rotation) is not satisfied in many instances. Under these circumstances it is unjustifiable to neglect the terms containing the squares and products of the rotations in the strain-displacement relations. Furthermore, the linear equilibrium equations are no longer valid and nonlinear terms consistent with the inclusion of rotations in the strain-displacement relations should be retained. Thus, stresses that multiply rotations should not automatically be dropped in deference to those that appear linearly in the equilibrium equations.

Geometric nonlinearity can exist independently of physical nonlinearity since small shears and elongations do not imply small angles of rotation. Problems requiring the consideration of geometric nonlinearity alone include the question of stability of elastic equilibrium, the deformation of bodies having initial stresses, large deflection of beams, plates and shells, and torsion and bending in the presence of axial forces. For these situations, the effect of geometric nonlinearity must be taken into account not only in the strain displacement relations, but in determining changes in the length of line elements, and in formulating the conditions of equilibrium of the volume element. In addition, if the magnitudes of the strains become too large, it then becomes necessary to include material nonlinearity through the stress-strain relations.

In the following, the procedure developed for material nonlinearity is expanded to include geometric nonlinearity. Although only elastic perfectly-plastic results are given, the method is equally applicable and easily adaptable to strain-hardening behavior using the procedure outlined in the previous section. Representative structures chosen to illustrate the significant features of combined geometric and material nonlinearity are the restrained beam and the circular arch.

Martin (Reference 6) has presented an incremental numerical method, based on the direct stiffness approach, which is generally applicable for the treatment of problems involving geometric nonlinearity. This procedure approximates the nonlinear behavior by a sequence of linear steps. Either loading or displacement may be applied incrementally. This procedure also requires the introduction of an initial stress stiffness matrix, in addition to the conventional stiffness matrix, to account for the effects on the bending stiffness of the membrane loads generated as a consequence of geometric nonlinearity; that is, the effects of rotations on strains. Thus, the implementation of this matrix in addition to the initial strain matrix represents the required modifications for the development of an incremental procedure to account for both types of nonlinearity.

A general development of the matrices discussed above and the method of solution to the problem of combined nonlinearity is obtained by following the procedure as outlined in Reference 6 with modifications associated with the inclusion of plasticity. The total elastic strain may be written as the sum of three components; i.e.,

$$\mathbf{e}^{e} = \mathbf{e}^{o} + \underbrace{\Delta\mathbf{e}^{T} - \Delta\epsilon}_{\Delta\mathbf{e}^{e}} \tag{28}$$

where $\mathbf{e}^{o}$ is the initial elastic strain vector (equal to P_0/AE for the beam column, and related to the initial stresses σ_x^o, σ_y^o, τ_{xy}^o for the two dimensional plate problem). The vector $\Delta\mathbf{e}^{T}$ is the additional total strain developed within the increment of load. This strain increment is related to the increments of displacement through the strain-displacement relations which must now include the nonlinear rotation terms. For a beam column element, this relationship is given by

$$\Delta e^{T} = \frac{d(\Delta u)}{dx} + \frac{1}{2}\left(\frac{d(\Delta w)}{dx}\right)^2 - z\,\frac{d^2(\Delta w)}{dx^2} \tag{29}$$

where Δu and Δw represent the increments in the axial and lateral displacements of the middle surface of the beam. The usual Bernoulli-Euler kinematic beam theory assumptions were made to obtain Equation 29. The first term in the above equation represents the extension of the centerline of the beam, the second term is the contribution to the extensional strain due to lateral deflection (the rotation term), and the last term is the conventional bending strain term arising from the condition that normals to the neutral axis should remain after deformation straight and normal to the centerline and unextended. The corresponding strain-displacement relations for a plate are

$$\Delta e_x^T = \frac{\partial(\Delta u)}{\partial x} + \frac{1}{2}\left(\frac{\partial(\Delta w)}{\partial x}\right)^2 - z\,\frac{\partial^2(\Delta w)}{\partial x^2}$$

$$\Delta e_y^T = \frac{\partial(\Delta v)}{\partial y} + \frac{1}{2}\left(\frac{\partial(\Delta w)}{\partial y}\right)^2 - z\,\frac{\partial^2(\Delta w)}{\partial y^2} \qquad (30)$$

$$\Delta \gamma_{xy}^T = \frac{\partial(\Delta u)}{\partial y} + \frac{\partial(\Delta v)}{\partial x} + \frac{\partial(\Delta w)}{\partial x}\,\frac{\partial(\Delta w)}{\partial y} - 2z\,\frac{\partial^2(\Delta w)}{\partial x\,\partial y}$$

The functional form for the increments in displacement for the beam column is chosen to be identical to that given in Equations 1 and 4 for the total displacement; that is,

$$\Delta w(x) = \sum_{i=1}^{2}\left[H_{0i}^{(1)}(x)\,\Delta w_i + H_{1i}^{(1)}(x)\,\Delta w_{,x_i}\right]$$

$$\Delta u(x) = \sum_{i=1}^{2} H_{0i}^{(0)}(x)\,\Delta u_i \qquad (31)$$

where the definitions of the Hermitian polynomials may be obtained by comparing corresponding terms in Equations 1, 4, and 31. A representation identical to that given in Reference 9 may be used for the increment of lateral displacement for the plate element. The incremental relationship between total strain and generalized nodal displacements is obtained by taking appropriate derivatives of the assumed displacement functions.

The increment in elastic strain energy from an initial elastic strain state, $\mathbf{e}^o$, may be written as

$$\Delta U = \iiint_V \left[\int_{\mathbf{e}^o}^{\mathbf{e}^o + \Delta \mathbf{e}^e} \boldsymbol{\sigma}'\, d\mathbf{e}^e\right] dV \qquad (32)$$

Integrating the above equation between the prescribed limits of strain and using the following relations:

$$\sigma = E \quad e^{e}$$
$$\sigma^{o} = E \quad e^{o}$$

and

$$\Delta e^{e} = \Delta e^{T} - \Delta \epsilon,$$

we can write the increment of strain energy as

$$\Delta U = \frac{1}{2} \iiint_{V} \Delta e^{T'} E \, \Delta e^{T} \, dV - \iiint_{V} \Delta e^{T'} E \, \Delta \epsilon \, dV + \iiint_{V} \sigma^{o'} \Delta e^{T} \, dV + \frac{1}{2} \iiint_{V} \Delta \epsilon' E \, \Delta \epsilon \, dV - \iiint_{V} \sigma^{o'} \Delta \epsilon \, dV \tag{33}$$

Only those terms in the above equation that contain Δe^{T}, which is a function of the increment of nodal displacement, will contribute to the incremental load-deflection-initial strain relationship. The remaining terms are arbitrary constants. Upon neglecting higher order terms in the increments of displacement, the first term in Equation 33 leads to the conventional stiffness matrix. The second term yields the initial strain matrix, while the third term leads to the initial stress stiffness matrix. In the development of the latter matrix the work done by the in-plane stresses and the generation of additional membrane stresses, resulting from the effects of geometric nonlinearity, are both taken to be zero during the application of an increment of lateral load. These considerations constitute the linearization of the procedure during an increment of load.

Consistent with the incremental procedure of the previous section, the increment of plastic strain may be written as

$$\Delta \epsilon^{i} = \epsilon^{i} - \epsilon^{i-1}$$

Substituting the above equation into Equation 33 and then making use of Castigliano's theorem leads to the following relation for an individual element:

$$\Delta P_{o}^{i} = k^{(0)} \Delta d_{o}^{i} + k^{(1)} \Delta d_{o}^{i} - \left[k^{*^{i}} \epsilon_{o}^{i} - k^{*^{i-1}} \epsilon_{o}^{i-1} \right] \tag{34}$$

where

$$k^{(0)} = \iiint_V W' E W \, dV,$$

the conventional stiffness matrix,

$$k^{(1)} = \iiint_V \tilde{W}' \sigma_0 \tilde{W} \, dV,$$

the initial stress stiffness matrix, and

$$k^* = \iiint_{V_p} W' E W_p \, dV,$$

the initial strain stiffness matrix. The matrix $\tilde{W}$ relates the increment of rotation to the increment of generalized nodal displacement and therefore represents the nonlinear contribution to the strain-displacement relations. The matrices W and W_p are the same as those used in the previous section.

A predictor-procedure must once again be used to obtain a solution because the location of the elastic-plastic boundary is not known a priori. Thus, the governing linear matrix equation is written in the following form:

$$\left(k^{(0)} + k^{(1)}\right) \Delta d_0^i = \Delta P_0^i + \Delta q^{i-1} \tag{35}$$

where Δq is defined in Equation 13, and must once again be retarded by one step in the solution procedure. Equation 35 is very nearly the same as Equation 13 used in Section II for the plastic bending analysis. However, because of the presence of geometric nonlinearity, the entire element stiffness matrix $k = k^{(0)} + k^{(1)}$ must be reformed at every step using current stress levels and geometry.

Thus the solution procedure requires that for a generic step, $k^{(0)}$ and $k^{(1)}$ are calculated by making use of the geometry and initial forces existing at the start of the step. The increment in the fictitious force, Δq, is calculated using current and the immediately preceding values of the location of the elastic-plastic boundary. An increment of load is then applied, and the corresponding displacement increments calculated from the total matrix equation obtained by assembling Equation 35 for each element. New internal forces are calculated

and total stresses, strains, and displacements are obtained by summing incremental values. The new location of the elastic-plastic boundary is determined from the total strain (or stress) distribution and the process is repeated until the maximum specified load level is reached or the structure fails.

SECTION IV

RESULTS

As a demonstration of the feasibility of the plastic bending analysis, application of the method has been made to some elementary, but representative sample structures. For two of these structures (a simply supported and a cantilevered beam), results from an exact solution to the governing differential equation, assuming elastic-ideally plastic material behavior, are available for comparison. As a consequence of assuming elastic-ideally plastic behavior, and since both of the structures are statically determinate, an analytic expression can be written which relates the depth of the elastic-plastic boundary to the applied load. The finite element analysis is initially applied to the beam structures using this relationship, thus providing a means of determining the validity of assumptions made in choosing such quantities as the displacement function, the plastic strain distribution, and the representation of the elastic-plastic boundary.

Figure 4a represents a nondimensionalized load versus central deflection curve for a uniformly loaded, simply supported beam. Six elements are used in the idealization of one-half of the beam. In this figure, w_0 is the center deflection, w_0^* is the center deflection at the maximum load for which the beam is entirely elastic, and ρ represents the nondimensional load parameter, given as

$$\rho = \frac{p}{p_0}\left(\frac{a}{t}\right)^2$$

Here, p is the applied load, and $p_0 = 4b\sigma_{yield}$. The results obtained from the finite element analysis compare quite favorably with corresponding results from the exact solution (Reference 10), as shown in Figure 4a. The collapse load, as determined from the near vertical slope of the load-deflection curve, is approximately three percent higher than the exact collapse load which occurs at a value of $\rho = 1$.

The progression of the elastic-plastic boundary through the thickness and in the plane of the element is shown in Figure 4b. From this figure it is seen that, although the depth of the boundary at plastic nodes is exact, the assumption associated with its distribution in the plane (i.e., linearly varying to adjacent nodes), may lead to discontinuities in the representation of its slope as evidenced in the figure for load values of $\rho = 1.00$ and $\rho = 1.03$. The appearance of these discontinuities indicates that the actual boundary lies between the nodes on the upper and lower surface of the beam. The error introduced by the assumption of a linearly varying boundary in the plane can be reduced by increasing the number of elements used in the idealization of the beam. Also to be noted in Figure 4b is the development of a fully plastic cross section located at the center of the beam at a load of $\rho = 1$. In a continuum analysis, the development of this fully plastic cross section is sufficient to cause collapse of this structure. However, in the finite element analysis, collapse does not occur until both cross sections of the element containing the center of the beam become fully plastic.

Results in the form of a nondimensionalized load versus tip-deflection curve for a uniformly loaded, cantilevered beam, are shown in Figure 5a. Elastic-ideally plastic material behavior was assumed. A comparison with results from an exact solution, shown as the solid curve in the figure, indicates good correlation up to the collapse load. For this problem, as for the simply supported beam, the depth of the elastic-plastic boundary can be directly related to the applied load. This relationship was used, once again, to obtain the results shown in the figure.

The progression of the elastic-plastic boundary, through the cross section and in the plane of the elements, is shown in Figure 5b. As indicated in the figure, the development of the boundary is much more localized for this structure than it was for the simply supported beam. Consistent with a continuum approach, collapse of this structure was indicated in the finite element analysis by the development of one fully plastic cross section at the root of the cantilever.

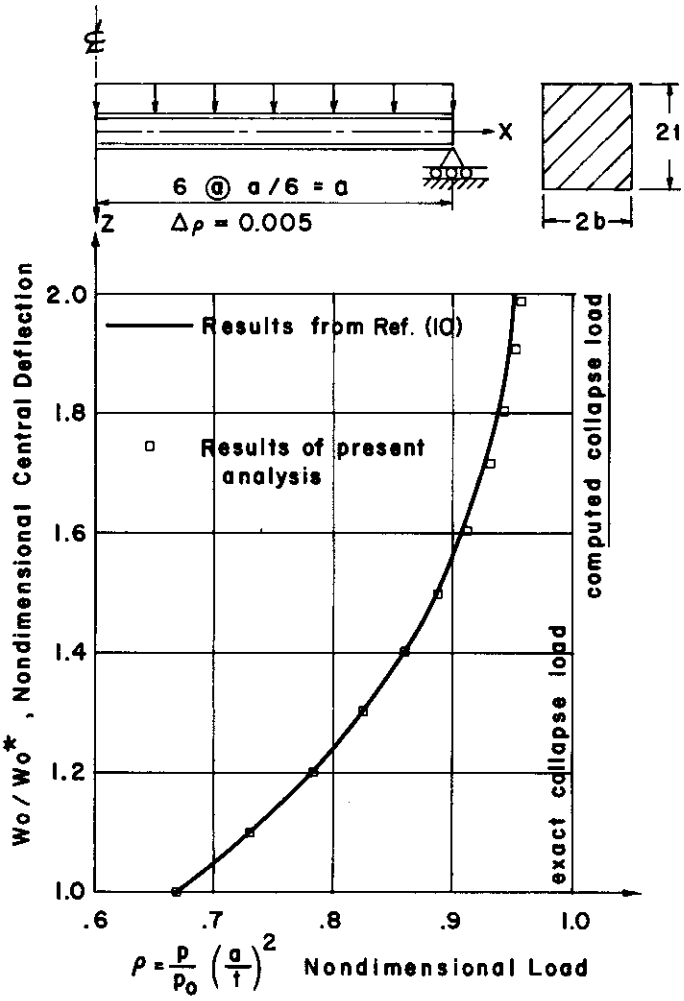

Figure 4a. Load Versus Deflection of a Simply Supported Beam

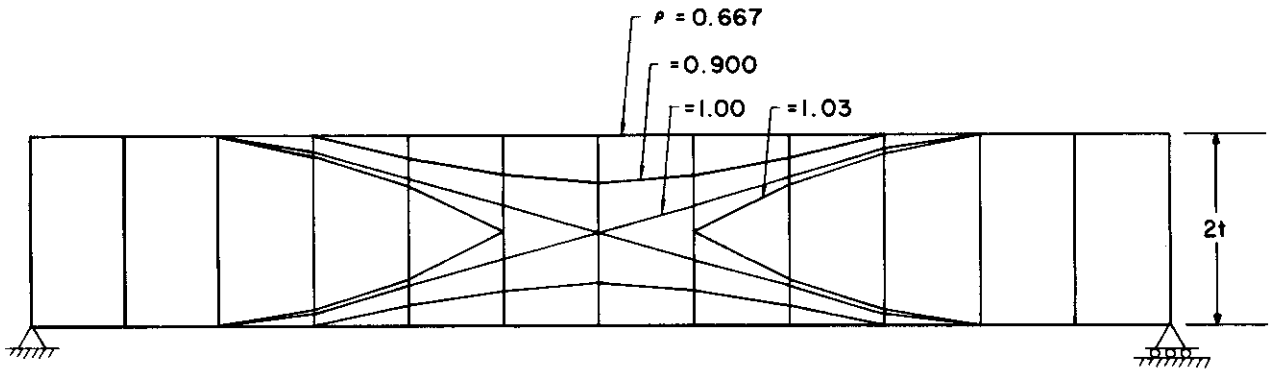

Figure 4b. Progression of Elastic-Plastic Boundary: Simply Supported Beam

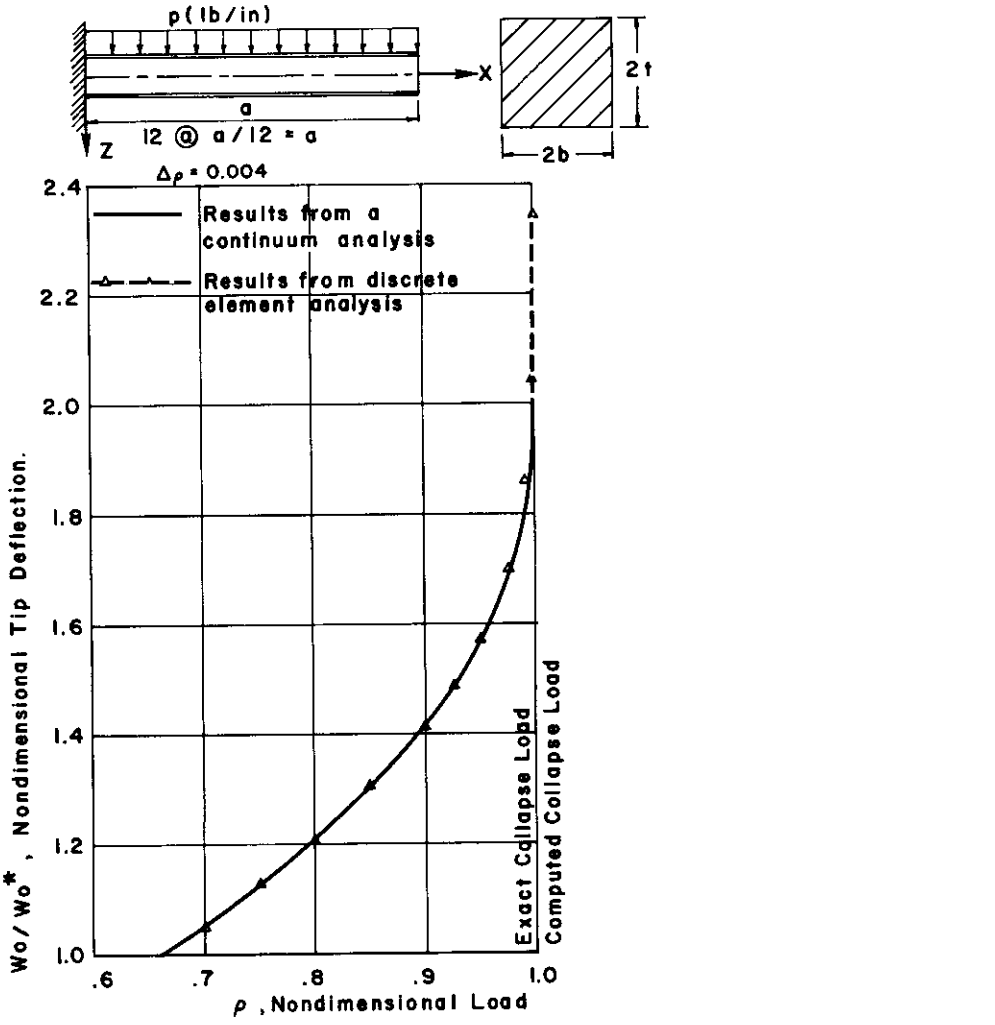

Figure 5a. Load Versus Deflection of a Cantilevered Beam

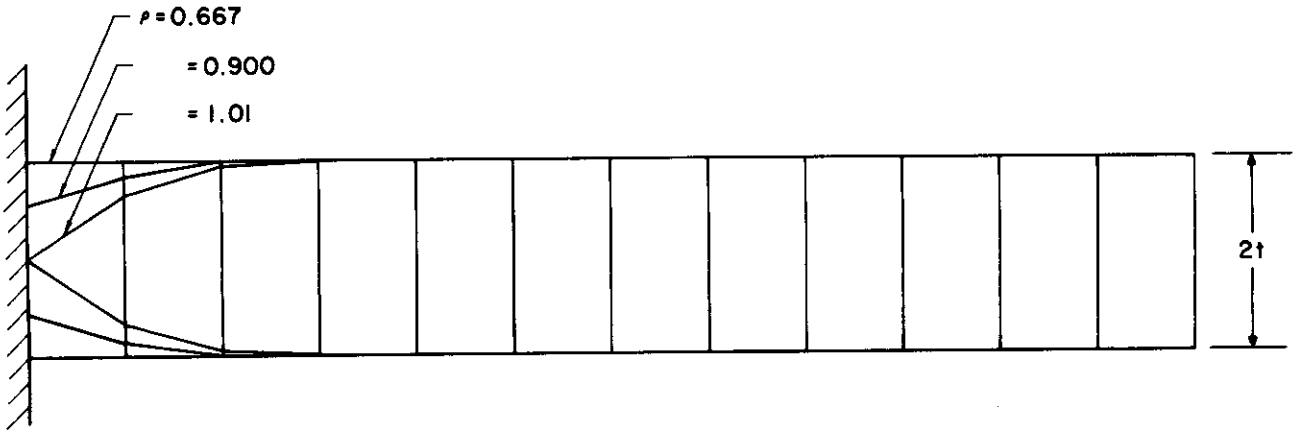

Figure 5b. Progression of Elastic-Plastic Boundary Cantilever Beam

For both the simply supported beam and the cantilevered beam, as previously mentioned, an exact relationship between the depth of the elastic-plastic boundary at nodes in the plastic range and the applied load was used to obtain results using the finite element analysis. The justification for using this relationship, which admittedly does not exist for most structures of interest, was to check the validity of assumptions made in choosing such quantities as the displacement function, the plastic strain distribution, and the representation of the elastic-plastic boundary. As indicated by the previous results, the use of these assumptions for the finite element analysis appears to be justified.

Since, in general, the depth of the elastic-plastic boundary is not known at the current load step, results for the cantilevered beam were recomputed and a load-deflection curve obtained, by using an approximate value for the depth of the elastic-plastic boundary which is shown in Figure 6. The value of the depth of the boundary used for any increment of load is based on the total strain distribution determined at the end of the previous load increment. The use of this procedure cannot lead to the development of a fully plastic cross section. Consequently, it is assumed that a fully plastic cross section exists at a node when plasticity has developed a specified amount through the thickness. The deflections and the slope of the load-deflection curve for this structure, increase quite rapidly beyond a value of load for which plasticity has developed through 80 percent of the end cross section. Thus, in the analysis this value was chosen as the criterion to determine the development of a fully plastic cross section. The degree of approximation obtained by using previous values of the depth of the boundary, when compared with the exact solution, is illustrated in Figure 6. As can be seen, the results compare favorably for most of the load range considered. The maximum divergence occurs in the vicinity of the collapse load, determined by using the exact boundary position. The error introduced by using the approximate position, for the prediction of the collapse load, is seven percent.

Results are also shown in Figure 6 for the cantilevered beam, for which strain hardening material behavior is assumed. These results, shown as the dotted curve, are compared with the corresponding results obtained by using elastic-ideally plastic behavior. The proximity of results for strain hardening and perfectly plastic behavior can be attributed to the use of Ramberg-Osgood strain hardening parameters, chosen to approximate the elastic-ideally plastic stress-strain curve. The slope of the load-deflection curve for strain hardening behavior illustrates that the beam still possesses some stiffness beyond the theoretical collapse load predicted by assuming perfectly plastic behavior.

Figure 7 illustrates the application of the procedure to a simply supported beam subjected to combined bending and axial loads. As previously discussed in Section III, the analysis for this problem requires the introduction of an initial stress stiffness matrix to account for the effects of the membrane load on the bending stiffness. The determination of the position of the elastic-plastic boundary relative to both the upper and lower surfaces is also required for this analysis. Results have been obtained for cases in which a uniform lateral load acts in conjunction with a constant tensile or compressive axial load, indicated in the figure by T = +1000 and T = -1000, respectively. These results are compared with the case of pure bending, indicated as T = 0. As seen in the Figure 7, the effect of the axial compressive load is to reduce the stiffness of the structure, and the tensile load increases the stiffness, when compared to the case of pure bending. A solution to this problem by using a continuum analysis similar to the one developed for pure bending in the plastic range does not appear to be available for comparison. For the case of the compressive axial load, the lateral load was incremented to a value that resulted in the failure of the structure. This failure is indicated in Figure 7 by the near vertical slope of the load-deflection curve. It should be noted that, for this problem, it was not necessary to develop a completely plastic cross section for collapse to occur. The reduction of the stiffness, caused by the axial compressive load and the progression of the elastic-plastic boundary through only a portion of the thickness, was sufficient to cause failure. This type of failure is associated with plastic buckling rather than the formation of a mechanism.

Application of this procedure has been made to a simply supported, uniformly loaded, square plate. Using a 36-element idealization to represent the quarter panel, load versus central deflection curves for this structure, assuming elastic-ideally plastic and elastic-strain hardening material behavior, are shown in Figure 8. Once again, as in the case of the beam, the proximity of results for both types of material behavior is attributable to the choice of strain hardening parameters that approximate elastic-ideally plastic material behavior.

The collapse load for this structure, determined by assuming elastic-ideally plastic material behavior, is the value of the load at which the pattern of fully plastic elements forms a mechanism of failure. The pattern of the development of the plastic region in the plane of the plate, and the progression of the boundary through the thickness of the plate, is shown in Figures 9a and 9b, respectively. In Figure 9a the cross-hatched area represents those regions of the plate in which plasticity has developed to some degree less than 80 percent through the cross section. The shaded area represents those regions in which plasticity has developed to a depth greater than 80 percent through the thickness. A consideration of the latter region as being fully plastic leads to the development of a mechanism of collapse

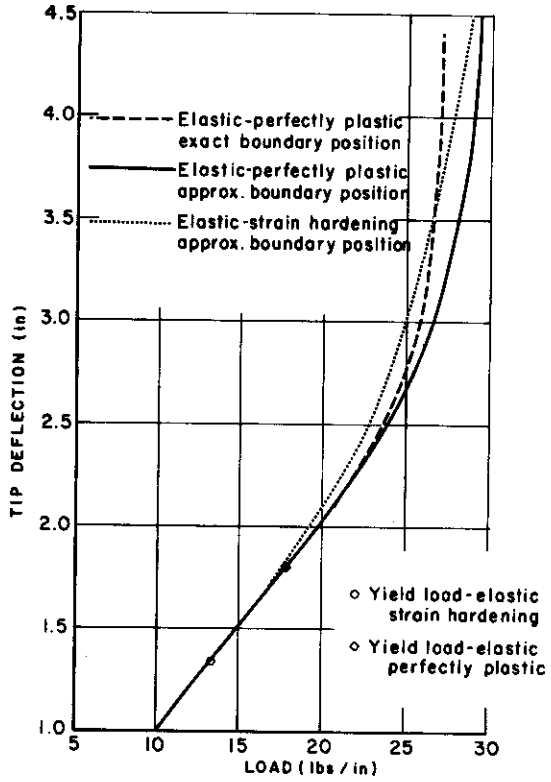

Figure 6. Load Versus Tip Deflection of Cantilever Beam

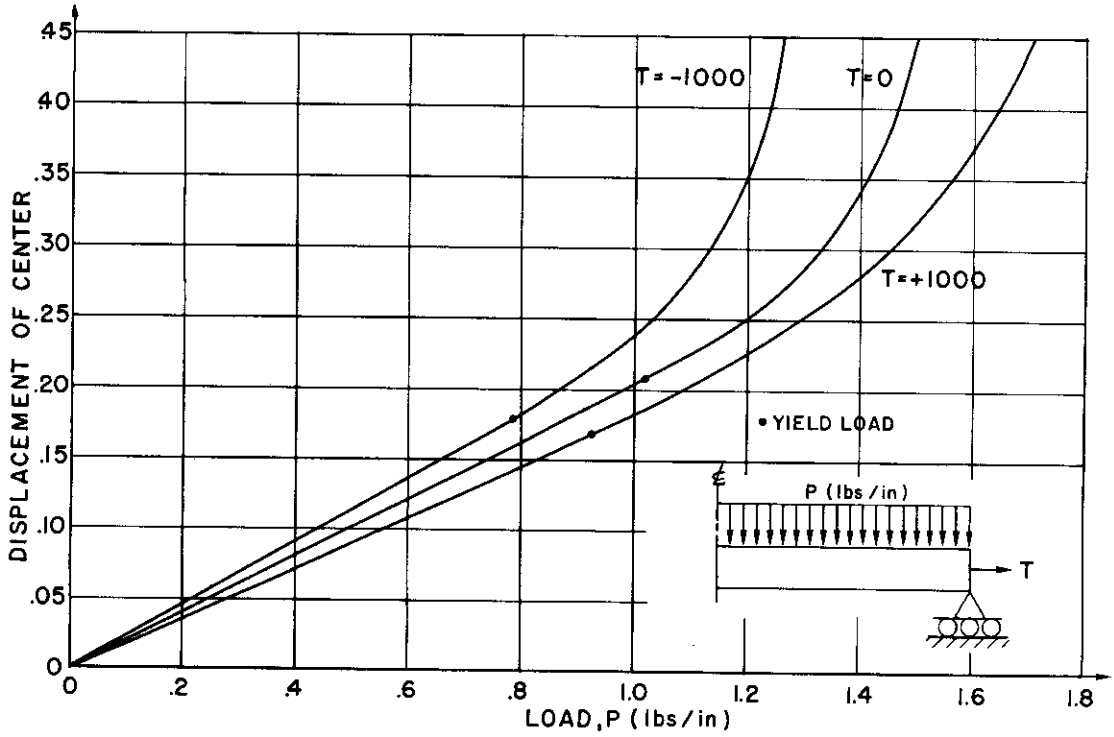

Figure 7. Simply Supported Beam Subjected to Combined Bending and Axial Loads

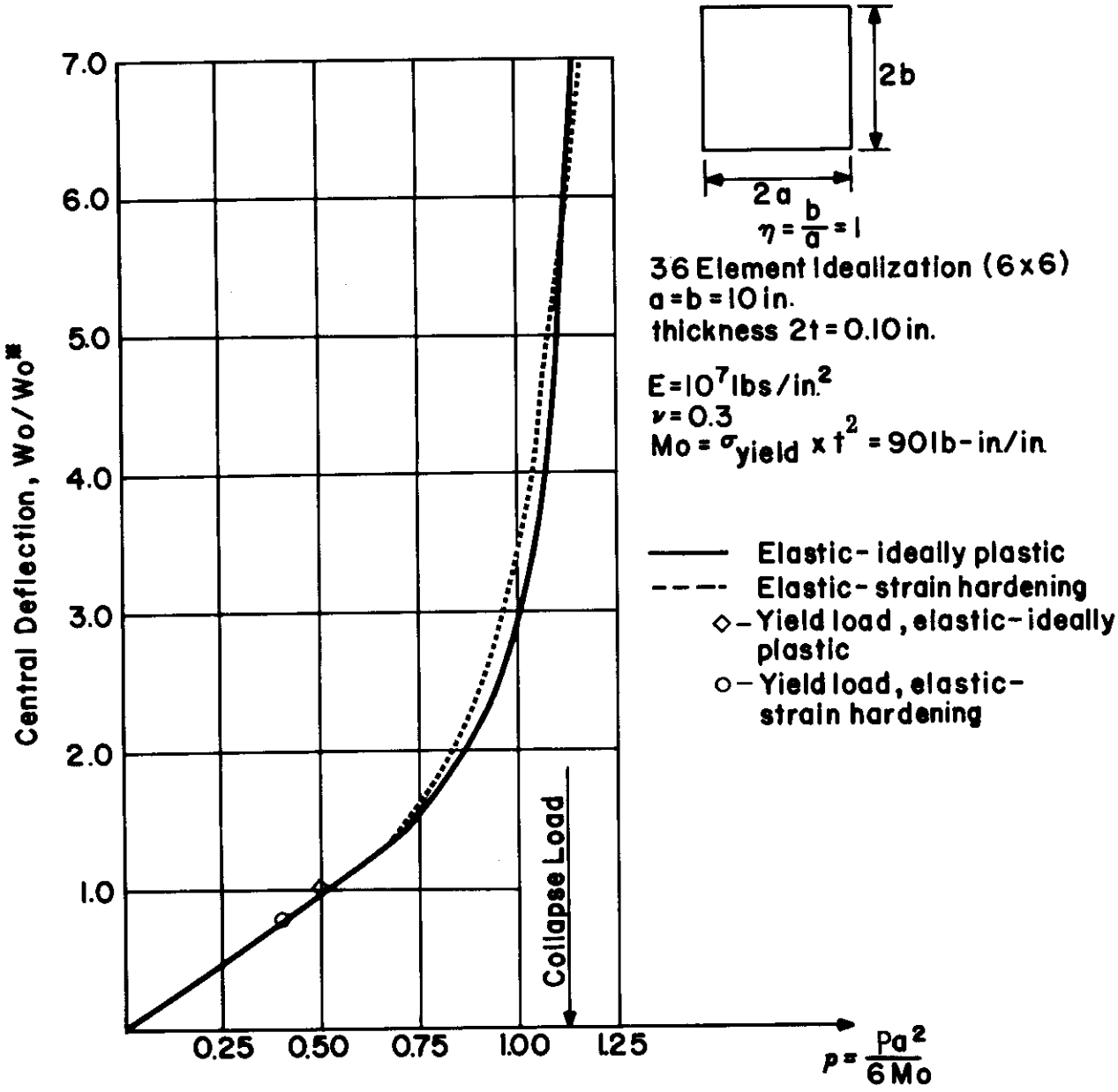

Figure 8. Load Versus Central Deflection of a Uniformly Loaded Simply Supported Square Plate

formed along the diagonals of the square plate, as shown in Figure 9a. As in the case of the beam, this criterion is necessary because the depth of the boundary, as computed from the total strains, cannot lead to the development of a fully plastic section.

The pattern of development of the plastic region in the plane of a narrow rectangular plate ($\eta = 0.3$) and the progression of the boundary through the thickness across the length and width of the plate, is shown in Figures 10a through 10c, respectively. In Figure 10a the 80 percent criterion was once again used to determine the pattern of fully plastic sections in forming the collapse mechanism. From this figure it is evident that the sections along the collapse pattern do not all lie on the diagonals of the plate.

A comparison of upper bound solutions for the load carrying capacities of rectangular plates of various aspect ratios is shown in Figure 11. The solid curve represents the solution obtained using the von Mises yield criterion in conjunction with assumed collapse pattern (1), shown in Figure 11. The dotted curve, obtained from Reference 12, represents the upper bound solution obtained using the Tresca yield condition, together with assumed collapse pattern (2). Results from the finite element analysis are represented by the solid circles. The finite element results indicate that the displacement pattern (2) is a more accurate representation of the collapse mechanism than is pattern (1). An upper bound solution using the second displacement pattern with the von Mises yield condition is shown as the dashed curve in Figure 11. The results from the present analysis compare favorably with this latter solution and are slightly below it except for extremely low aspect ratios. For such narrow plates, the use of the 80 percent criterion in conjunction with the depth of the elastic-plastic boundary, calculated from the total strain distribution of the previous step, is not adequate. A relaxation of the 80 percent criterion, based on a careful examination of the load deflection history, appears to be warranted. In addition, a possible alternative might be the incorporation of an iterative procedure in the method of solution.

To illustrate the procedure associated with geometric nonlinearity and combined material and geometric nonlinearity, a simply supported, restrained beam, subjected to a uniform vertical load, is considered. Load versus central deflection curves, obtained for purely elastic and for elastic-ideally plastic material behavior are shown in Figure 12a. Results assuming elastic behavior from the finite element analysis and exact results from Reference 13 are shown as the dotted curve in the figure. Load versus deflection curves, assuming plastic behavior are presented for idealizations involving 6, 12, and 24 elements for one-half of the beam. Differences in the results for these idealizations only appear after the

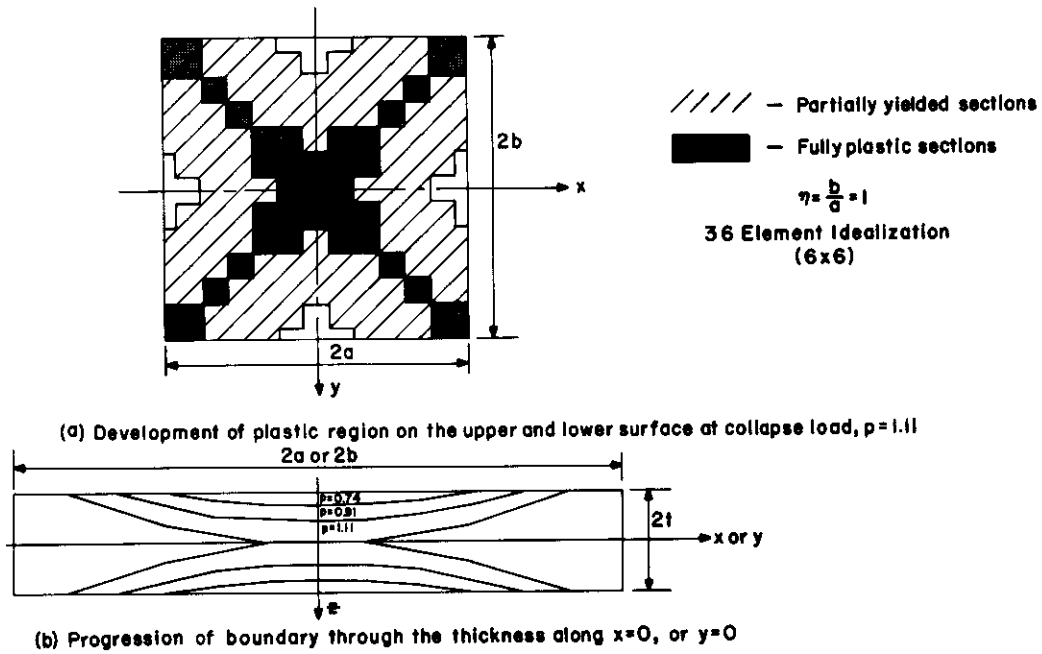

Figure 9. Progression of Elastic-Plastic Region for Simply-Supported, Uniformly Loaded, Square Plate

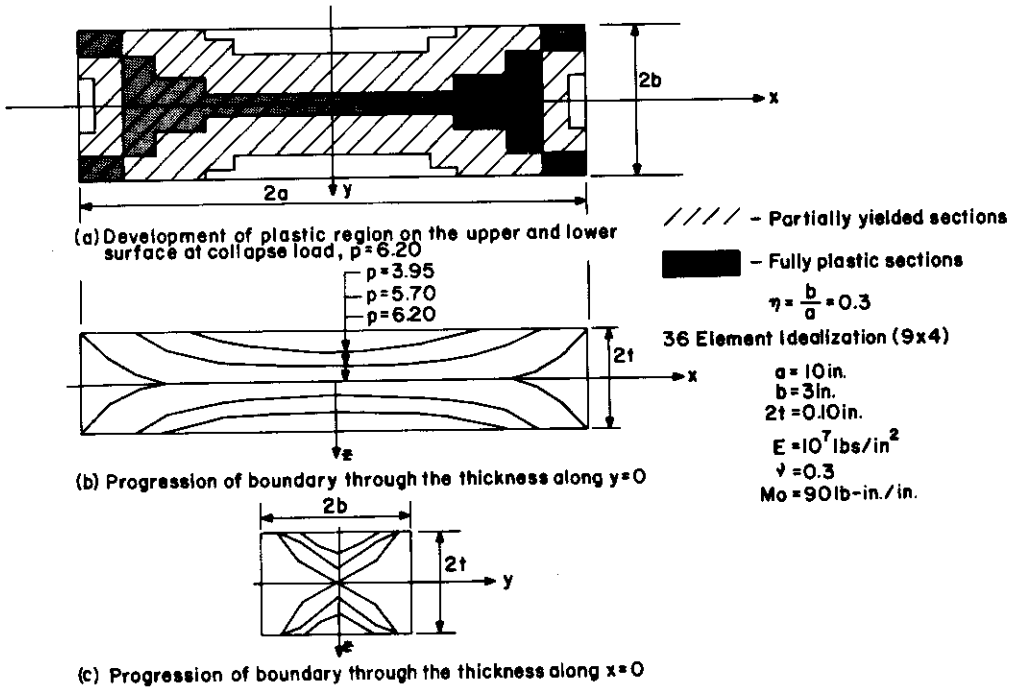

Figure 10. Progression of Elastic-Plastic Region for Simply-Supported, Uniformly Loaded Rectangular Plate

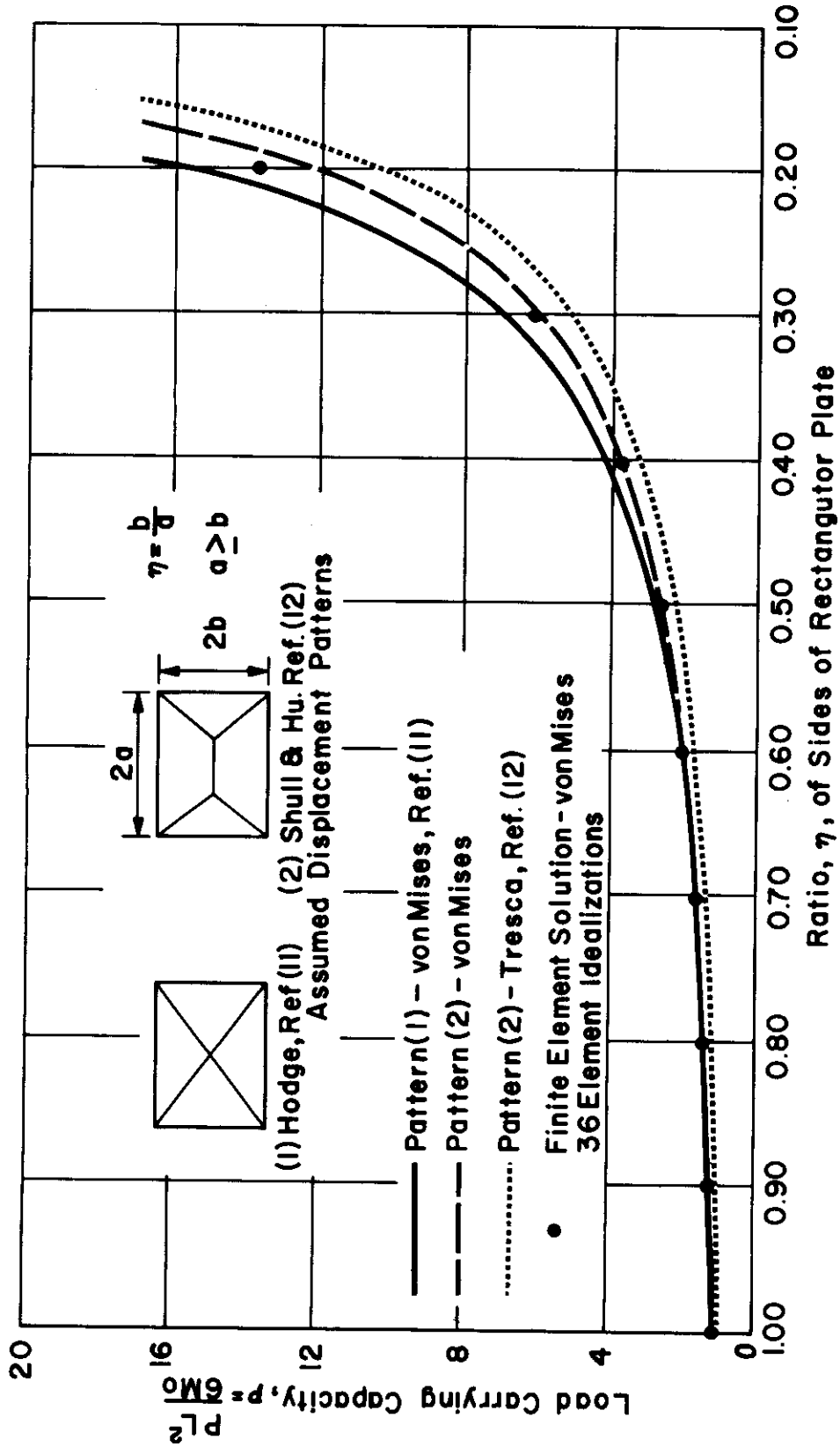

Figure 11. Comparison of Upper Bounds on Load Carrying Capacities of Rectangular Plates

end sections at the supports become fully plastic. Deflections beyond the value of load at which this occurs increase quite rapidly, and collapse occurs shortly thereafter with the development of another fully plastic cross section. The counterbalancing effect of geometric and material nonlinearity is vividly depicted in Figure 12a by the region of the load-deflection curve which is very nearly linear.

Figure 12b illustrates the growth of the plastic regions of the restrained beam. The dotted line at P = 179 lb/in. indicates the jump in the representation of the plastic region, when the end section becomes fully plastic.

The load-deflection history of a circular arch subjected to a concentrated load is shown in Figure 13. The elastic buckling load compares favorably with that obtained in Reference 5. Load versus center deflection curves, obtained by assuming elastic-ideally plastic material behavior, are shown for two values of yield stress. The onset of collapse for this structure is appreciably hastened with the introduction of plasticity. This is attributable to the reduction of the stiffness of the structure resulting from the complementary effects of geometric and physical nonlinearity. As in the case of the uniformly loaded beam subjected to a constant axial compressive load, the development of a fully plastic cross section was not necessary for collapse to occur.

Figure 14 illustrates the load-deflection histories of the same arch as that used in Figure 13, now subjected to a uniform load distribution. Once again it is seen that the effect of plasticity considerably reduces the collapse load of the structure from its elastic buckling load.

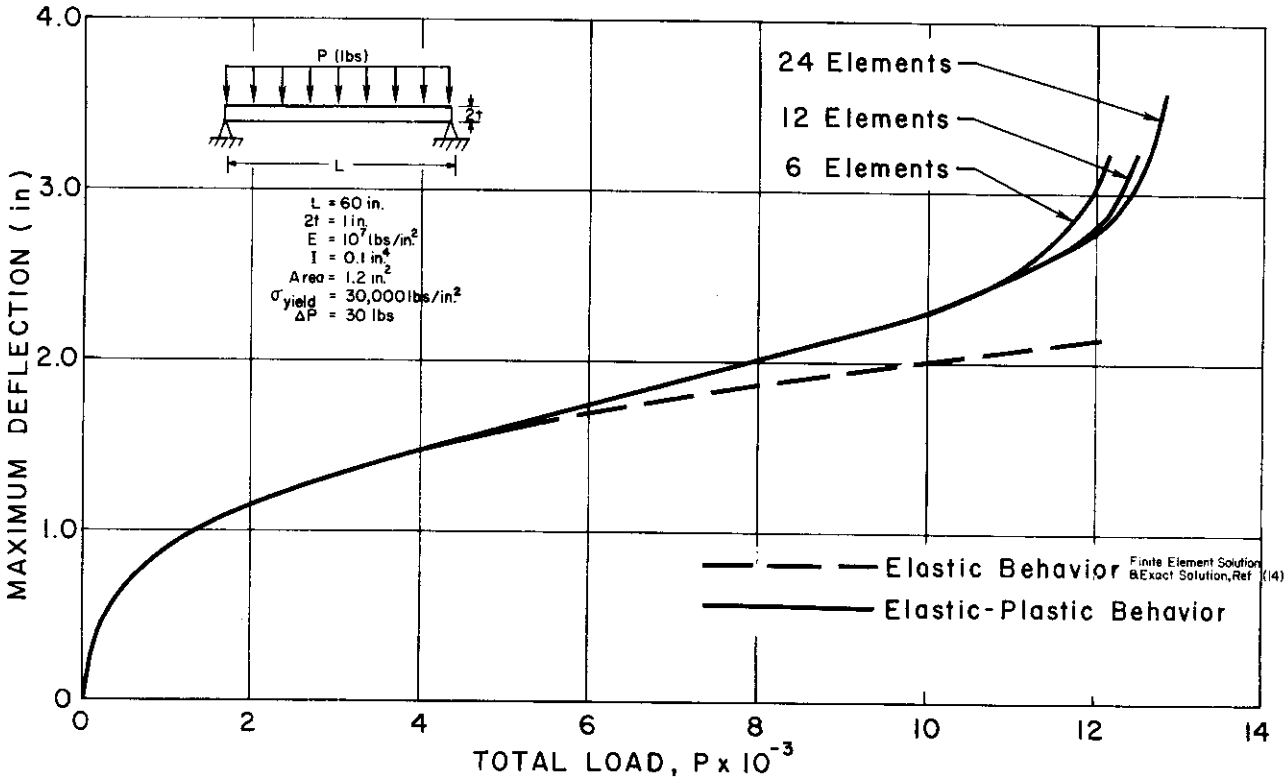

Figure 12a. Elastic-Plastic Response of a Restrained Beam

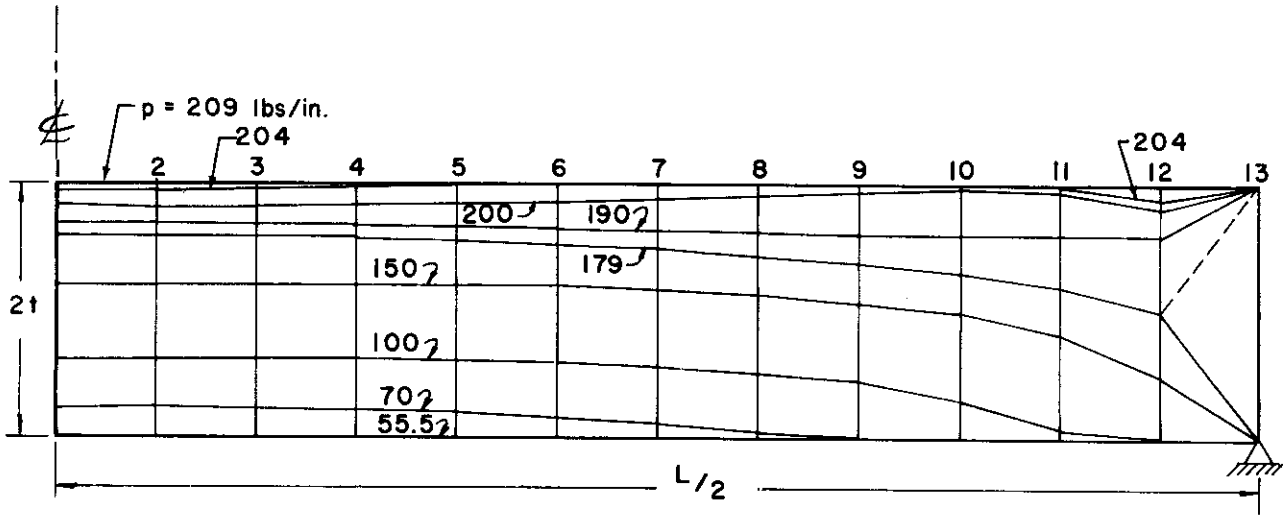

Figure 12b. Progression of Elastic-Plastic Boundary in Restrained Beam for Increasing Load

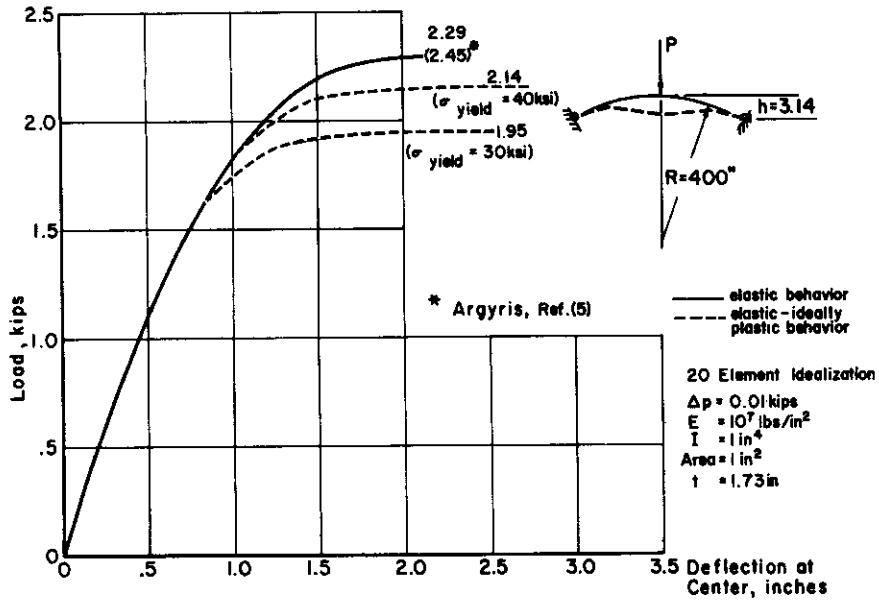

Figure 13. Load Versus Central Deflection for a Simply Supported Arch Subjected to a Concentrated Load

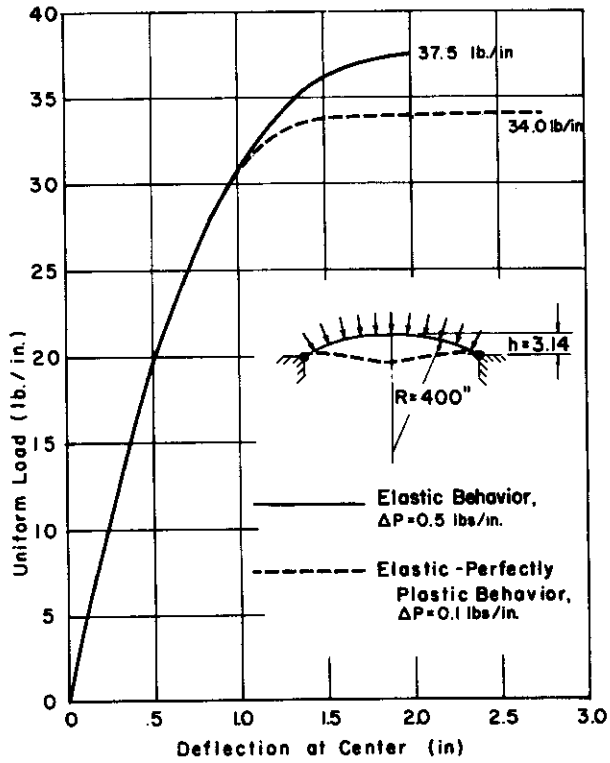

Figure 14. Load Versus Central Deflection of a Simply Supported Arch Subjected to a Uniform Load

SECTION V

SUMMARY AND CONCLUSIONS

A finite element method is presented that can account for material nonlinearity, alone, or in combination with geometrically nonlinear behavior for the out-of-plane bending analysis of structures. The initial strain concept is implemented into the finite element analysis, formulated within the framework of the direct stiffness method, to account for the effects of plasticity. These effects are introduced into the analysis as a fictitious load vector to be combined with the actual applied load. Thus, the method of analysis can be readily incorporated into existing finite element procedures.

Application of the method, illustrating the plastic behavior of typical structures under pure bending, and bending in combination with applied axial loads, is presented. Results from the finite element analysis are compared with results from analytical solutions, where possible, for beam and plate structures. Good correlation is indicated for the load-deflection characteristics of these structures as well as for the prediction of plastic collapse loads. In addition, with the generation, or application of compressive membrane stresses, the present procedure is capable of predicting failure resulting from a combination of plastic collapse and buckling. The correlation of results and the numerical stability of the procedure as applied to the sample problems substantiates the assumptions associated with the functional representation of the elastic-plastic boundary and the distribution of the plastic strain within each element, in addition to the use of the predictor form of the solution procedure.

Since the phenomenon of plastic deformations may itself lead to large displacements and rotations, the treatment of effects arising from geometric nonlinearity assumes particular significance in the solution of many important problems. Consequently, the plastic bending analysis was combined with a method capable of accounting for geometrically nonlinear behavior. This combined procedure was applied to a restrained beam and a simply supported circular arch. In the beam, the effects of geometric nonlinearity act counter to the reduction of stiffness caused by the progressive development of plasticity. Failure of this structure occurs only after the development of fully plastic cross sections. For the circular arch, the effects of both types of nonlinearity are complementary, and failure occurs as a plastic buckling phenomenon.

Acknowledgement

The authors gratefully acknowledge the work of Joseph S. Miller in programming the analysis.

SECTION VI

REFERENCES

1. Isakson, G., Armen, H., Jr., and Pifko, A., Discrete-Element Methods for the Plastic Analysis of Structures, NASA Contractors Report, CR-803, October 1967.

2. Lansing, W., Jensen, W. R., and Falby, W., "Matrix Analysis Methods for Inelastic Structures," Proc. of Conf. on Matrix Methods in Structural Mechanics, Wright-Patterson AFB, Ohio, AFFDL-TR-66-80, October 26-28, 1965.

3. Pope, G. G., "The Application of the Matrix Displacement Method in Plane Elasto-Plastic Problems," Proc. of Conf. on Matrix Methods in Structural Mechanics, Wright-Patterson AFB, Ohio, AFFDL-TR-66-80, October 26-28, 1965.

4. Marcal, P. V., "A Comparative Study of Numerical Methods of Elastic-Plastic Analysis," AIAA Journal, Vol. 6, No. 1, January 1965, p. 157.

5. Argyris, J. H., "Continua and Discontinua," Proc. of Conf. on Matrix Methods in Structural Mechanics, Wright-Patterson AFB, Ohio, AFFDL-TR-66-80, October 26-28, 1965.

6. Martin, H. C., "On the Derivation of Stiffness Matrices for the Analysis of Large Deflection and Stability Problems," Proc. of Conf. on Matrix Methods in Structural Mechanics, Wright-Patterson AFB, Ohio, AFFDL-TR-66-80, October 26-28, 1965.

7. Popov, E. P., Khojesteh-Bakht, M., and Yaghmai, S., "Analysis of Elastic-Plastic Circular Plates," ASCE Journal, Engineering Mechanics Division, Vol. 93, No. EM6, pp. 49-65, December 1967.

8. Hodge, P. G., Jr., "Limit Analysis of Rotationally Symmetric Plates and Shells," Chapter 3, Prentice-Hall, Inc., 1963.

9. Bogner, F. K., Fox, R. L., and Schmit, L. A., Jr., "The Generation of Inter-Element-Compatible Stiffness and Mass Matrices by the use of Interpolation Formulas," Proc. of Conf. on Matrix Methods in Structural Mechanics, Wright-Patterson AFB, Ohio, AFFDL-TR-66-80, October 26-28, 1965.

10. Prager, W. and Hodge, P. G., Jr., "Theory of Perfectly Plastic Solids," Chapter 2, John Wiley & Sons, Inc., 1951.

11. Hodge, P. G., Jr., "Plastic Analysis of Structures," Chapter 10, McGraw-Hill Book Co., 1959.

12. Shull, H. E. and Hu, L. W., "Load-Carrying Capacities of Simply Supported Rectangular Plates," Journal of Applied Mechanics, Vol. 30, No. 4, Trans. ASME, Series E, p. 617, December 1963.

13. Timoshenko, S. and Woinowsky-Krieger, S., "Theory of Plates and Shells," Chapter 1, p. 4, McGraw-Hill Book Co., 1959.

14. Armen, H., Jr., Pifko, A., and Levine, H. S., "A Finite Element Method for the Plastic Bending Analysis of Structures," Grumman Research Department Report RE-347J, October 1968.

APPENDIX

INITIAL STRAIN STIFFNESS MATRICES FOR BEAM FINITE ELEMENTS

The initial strain stiffness matrices for a beam element in pure bending and for combined bending and membrane loading, are derived on the basis of the assumptions shown in Figures 1 and 2, and are given in integral form in Equation 10.

The matrix equation defining the fictitious nodal restoring forces in terms of the resulting initial strain stiffness matrix, is shown below for the pure bending of a beam with a rectangular cross section, represented as

$$\begin{Bmatrix} P_{z_i} \\ M_i \\ P_{z_j} \\ M_j \end{Bmatrix} = \frac{EI}{t^3} \begin{bmatrix} c_1/\ell & c_2/\ell \\ c_3 & c_4 \\ -c_1/\ell & -c_2/\ell \\ c_5 & c_6 \end{bmatrix} \begin{Bmatrix} \epsilon_{0i} \\ \epsilon_{0j} \end{Bmatrix} = k^* \epsilon_0 \tag{36}$$

where

$$c_1 = \frac{(\bar{z}_j - \bar{z}_i)^2}{20} + t^2 - \frac{\bar{z}_i(t + \bar{z}_i)}{2}$$

$$c_2 = \frac{9(\bar{z}_j - \bar{z}_i)^2}{20} + \frac{(\bar{z}_j - \bar{z}_i)(2\bar{z}_i + t)}{2} - t^2 + \frac{\bar{z}_i(t + \bar{z}_i)}{2}$$

$$c_3 = -\frac{(\bar{z}_j - \bar{z}_i)^2}{60} - \frac{(\bar{z}_j - \bar{z}_i)(2\bar{z}_i + t)}{12} + t^2 - \frac{\bar{z}_i(t + \bar{z}_j)}{2}$$

$$c_4 = \frac{(\bar{z}_j - \bar{z}_i)^2}{10} + \frac{(\bar{z}_j - \bar{z}_i)(2\bar{z}_i + t)}{12}$$

$$c_5 = \frac{(\bar{z}_j - \bar{z}_i)^2}{15} + \frac{(\bar{z}_j - \bar{z}_i)(2\bar{z}_i + t)}{12}$$

$$c_6 = \frac{7(\bar{z}_j - \bar{z}_i)^2}{20} + \frac{5(\bar{z}_j - \bar{z}_i)(2\bar{z}_i + t)}{12} - t^2 + \frac{\bar{z}_i(t + \bar{z}_i)}{2}$$

and P_z and M represent the fictitious restoring force in the lateral direction and moments, respectively. For this element, all $\bar{z}$'s are determined with respect to the median surface. Other quantities appearing in Equation 36 are defined in Figure 1.

The corresponding relations for the case of combined bending and membrane stresses are shown below:

$$\begin{Bmatrix} P_{z_i} \\ M_i \\ P_{x_i} \\ P_{z_j} \\ M_j \\ P_{x_j} \end{Bmatrix} = \frac{EI}{\ell^2 t^3} \begin{bmatrix} k^*_{11} & k^*_{12} & k^*_{13} & k^*_{14} \\ k^*_{21} & k^*_{22} & k^*_{23} & k^*_{24} \\ k^*_{31} & k^*_{32} & k^*_{33} & k^*_{34} \\ -k^*_{11} & -k^*_{12} & -k^*_{13} & -k^*_{14} \\ k^*_{51} & k^*_{52} & k^*_{53} & k^*_{54} \\ -k^*_{31} & -k^*_{32} & -k^*_{33} & -k^*_{34} \end{bmatrix} \begin{Bmatrix} \epsilon^U_{0i} \\ \epsilon^U_{0j} \\ \epsilon^L_{0i} \\ \epsilon^L_{0j} \end{Bmatrix} \tag{37}$$

where

$$k^*_{11} = -(\ell^3/40)c_1 + (\ell/4)c_3$$

$$k^*_{12} = -(9\ell^3/40)c_1 - (\ell^2/4)c_2 - (\ell/4)c_3$$

$$k^*_{13} = -(\ell^3/40)c_4 + (\ell/4)c_6$$

$$k^*_{14} = -(9\ell^3/40)c_4 - (\ell^2/4)c_5 - (\ell/4)c_6$$

$$k^*_{21} = (\ell^4/120)c_1 + (\ell^3/24)c_2 + (\ell^2/4)c_3$$

$$k^*_{22} = -(\ell^4/20)c_1 - (\ell^3/24)c_2$$

$$k^*_{23} = (\ell^4/120)c_4 + (\ell^3/24)c_5 + (\ell^2/4)c_6$$

$$k^*_{24} = -(\ell^4/20)c_4 - (\ell^3/24)c_5$$

$$k^*_{31} = -(\ell^3/8)c_7 - (3\ell^2/8)c_8$$

$$k^*_{32} = -(\ell^3/4)c_7 - (3\ell^2/8)c_8$$

$$k^*_{33} = (\ell^3/8)c_9 + (3\ell^2/8)c_{10}$$

$$k^*_{34} = (\ell^3/4)c_9 + (3\ell^2/8)c_{10}$$

$$k^*_{51} = -(\ell^4/30)c_1 - (\ell^3/24)c_2$$

$$k^*_{52} = -(7\ell^4/40)c_1 - (5\ell^3/24)c_2 - (\ell^2/4)c_3$$

$$k^*_{53} = -(\ell^4/30)c_4 - (\ell^3/24)c_5$$

$$k^*_{54} = -(7\ell^4/40)c_4 - (5\ell^3/24)c_5 - (\ell^2/4)c_6$$

and

$$c_1 = \left(\bar{z}^U_j - \bar{z}^U_i\right)^2 / \ell^2$$

$$c_2 = -\left(\bar{z}^U_j - \bar{z}^U_i\right)\left(3t - 2\bar{z}^U_i\right) / \ell$$

$$c_3 = -\bar{z}^U_i\left(3t - \bar{z}^U_i\right)$$

$$c_4 = -\left(\bar{z}^L_j - \bar{z}^L_i\right)^2 / \ell^2$$

$$c_5 = \left(\bar{z}^L_j - \bar{z}^L_i\right)\left(t - 2\bar{z}^L_i\right) / \ell$$

$$c_6 = 2t^2 + t\bar{z}^L_i - \bar{z}^{L\,2}_i$$

$$c_7 = \left(\bar{z}^U_j - \bar{z}^U_i\right) / \ell$$

$$c_8 = \bar{z}^U_i$$

$$c_9 = \left(\bar{z}^L_j - \bar{z}^L_i\right) / \ell$$

$$c_{10} = \bar{z}^L_i - 2t$$

The terms, P_{x_i} and P_{x_j}, represent the fictitious restoring forces in the axial direction. Here all $\bar{z}$'s are measured with respect to the upper surface of the beam. All other quantities appearing in Equation 37 are defined in Figure 2.